Structural basis of membrane-targeting by the Dock180 family of RhoGEFs

Lakshmanane Premkumar[1,2], Andrey A. Bobkov[1,2], Manishha Patel[3], Lukasz Jaroszewski[2], Laurie A. Bankston[1,2], Boguslaw Stec[1,2], Kristiina Vuori[1], Jean-Francois Côté[3], and Robert C. Liddington[1,2]

SUPPLEMENTARY DATA

Figure S1. The surface loops of DHR-1

(A) and (B) Differences between surface loops in 2 independent copies within the DHR-1 crystals. Loops L1 **(A)** and L3 **(B)** are overlaid, with selected side chains shown. Analogous loops are typically poorly ordered in C2 domains, but in DHR-1, L1 (441-444) and L2 (Molecule A: 520-524; and Molecule B: 518-524) are connected at the 0.7σ and 0.6σ contour levels in a CNS $2F_o - F_c$ density map. Residue labeling is for the conformation shown in yellow.

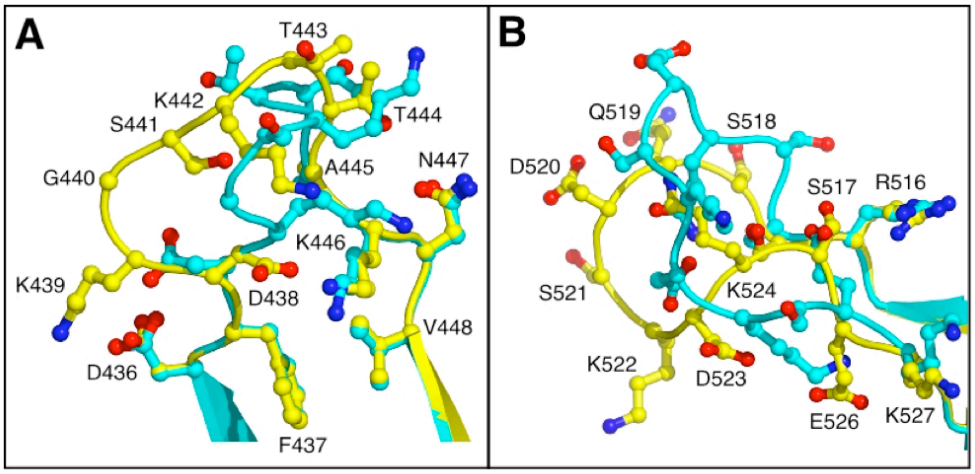

(C) Simulated-annealing omit map (stereo image) of Molecule A. Annealing at 1000 K in 'torsion dynamics' mode was performed with CNS, in which residues K446 and H515 (a 3.5 Å sphere around these residues) were omitted from phasing. The 2mFo-DFc map is displayed around the labeled residues at a 1.0 σ contour.

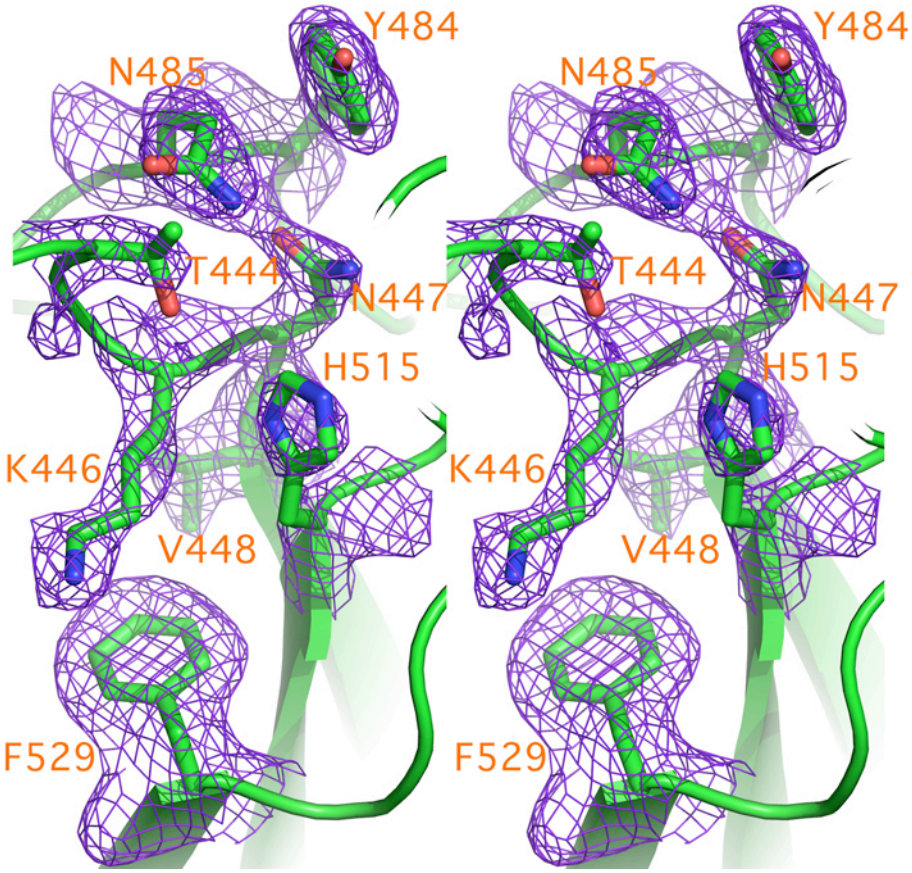

Figure S2. DHR-1 Structural homologs assessed by DALI (Holm et al, 2008). Top 41 closest homologs (unique sequences), ranked by "Z-score". Z-scores above 6 are considered 'highly significant'. Columns are: Rank, PDB code, "Z-score", RMS difference on Cα for the given number of aligned residues (# align). %id = % identity for the aligned residues.

Rank	PDB	Z	RMSD	#align	%id	PROTEIN
1:	2isd	13.3	2.1	121	12	PHOSPHOINOSITIDE PHOSPHOLIPASE C
2:	2enq	12.9	2.8	143	10	PtdIns(4,5) 3-KINASE ALPHA
3:	2qzq	12.9	2.4	129	14	DORSALIZATION ASSOCIATED PROTEIN
4:	1qas	12.8	2.2	118	12	PHOSPHOLIPASE C DELTA-1
8:	2nsq	12.7	2.0	119	16	E3 LIGASE NEDD4-LIKE PROTEIN
9:	1e8x	12.6	2.3	127	12	PtdIns(4,5) 3-KINASE GAMMA
10:	1cjy	12.4	2.0	115	12	CYTOSOLIC PHOSPHOLIPASE A2
11:	2nq3	12.3	2.7	119	15	ITCHY HOMOLOG E3 LIGASE
12:	1rlw	12.3	1.7	112	13	PHOSPHOLIPASE A2
13:	2cjt	12.0	2.6	117	14	UNC-13 HOMOLOG A
14:	3jzy	12.0	1.9	111	11	INTERSECTIN 2
15:	2dmh	11.6	2.2	114	14	MYOFERLIN
16:	2ep6	11.4	2.0	112	13	MCTP2
17:	1gmi	10.8	2.5	110	8	PROTEIN KINASE C, EPSILON
18:	1uov	10.4	2.2	113	14	SYNAPTOTAGMIN I
19:	2fk9	10.2	2.4	108	11	PROTEIN KINASE C, ETA
20:	1tjx	10.1	2.4	113	15	SIMILAR TO SYNAPTOTAGMININ/P65
21:	1dqv	10.0	3.5	111	9	SYNAPTOTAGMIN III
22:	2dmg	9.8	2.6	116	10	KIAA1228 PROTEIN
23:	2uzp	9.8	3.0	116	9	PROTEIN KINASE C, GAMMA
24:	3fdw	9.8	2.6	109	15	SYNAPTOTAGMIN-LIKE PROTEIN 4
25:	1a25	9.8	2.8	114	10	PROTEIN KINASE C, BETA
26:	2bwq	9.8	1.9	101	13	RIM2 C2A
27:	1wfj	9.7	2.6	107	15	PUTATIVE ELICITOR-RESPONSIVE GENE
28:	2jqz	9.7	2.7	117	14	HSMURF2
29:	3fbk	9.5	3.6	119	12	REGULATOR OF G-PROTEIN SIGNALING 3;
30:	2k8m	9.5	2.3	110	13	PUTATIVE UNCHARACTERIZED PROTEIN
31:	2d8k	9.4	2.5	110	10	SYNAPTOTAGMIN VII
32:	2k3h	9.4	2.5	107	12	RABPHILIN-3A;
33:	1w15	9.1	2.1	102	14	SYNAPTOTAGMIN IV;
34:	2q3x	9.1	2.5	111	11	SYNAPTIC MEMBRANE EXOCYTOSIS REGULATOR
35:	2z0u	8.9	2.3	104	11	WW DOMAIN-CONTAINING PROTEIN 1
36:	2yrb	8.7	2.7	120	7	PROTEIN FANTOM;
37:	2enp	8.3	2.7	110	14	B/K PROTEIN;
38:	1rh8	7.9	2.7	105	12	PICCOLO PROTEIN
39:	2enj	7.3	3.0	102	14	PROTEIN KINASE C, THETA
40:	1wfm	7.1	3.1	106	12	SYNAPTOTAGMIN XIII
41:	1d5r	7.0	2.7	102	12	PHOSPHOINOSITIDE PHOSPHATASE PTEN

Figure S3. Structural and sequence comparisons between Dock1 DHR-1 domain and PtdIns 3-kinase (2ENQ).

A. Structure-based alignment from DALI, with secondary structure (H=helix; E=strand; L=loop) indicated. PtdIns 3-kinase has shorter insertions at the two insertions indicated. Sequence identity is 10%.

β2-β3 loop

```
DHR-1 NDIYVTLVQGDFDKGSKSTTAKNVEVTVSVYDEDGKRLEHVIFPGAGDEAISEYKSVIYY
2ENQ  SALRIKILCATVNVN-IRDIDRIYVRTGIYHGGEPLC----------DNVNTQRVP---
      LEEEEEEEEEELLLLLLLLLLLEEEEEEEEELLLLLLLLLEELLLLLLLLLEELLLLLL
```

```
DHR-1 QVKQPRWFETVKVAIPIEDVNRSHLRFTFRHRSSQDSKDKSEKIFALAFVKLMRYDGTT
2ENQ  -CSNPRWNEWLNYIYIPDLPRAARLCLSICSVKGRKGAKEEHCPLAWGNINLFDYYDTL
      LLLLLLLLEEEEEELLLLLHHHEEEEEEEEELLLLLLLLLLLLEEEEEEEELLLLLLLL
```

β7-β8 insertion

```
DHR-1 LRDGEHDLIVYKAEAKKLEDAATYLSLPSTKAELEEKSMQSLGSCTISKDSFQISTLVC
2ENQ  TLV--SGKMALNLWPVGLEDLNPIGVTGSNP----------------KETPCLEFDWF
      LLLEEEEELLEELLHHHHLLHHHHLLLLLLHHHHHLLLLLEELLEEELLLEEEEEEEEL
```

B. Structural overlay (stereo). Superposition of the DHR-1 C2 domain (violet) with the PI 3-kinase-γ C2 domain (gray). The HEAT/ARM repeats (magenta) found in the full-length structure of PtdIns 3-kinase-γ are also shown. Note that the helix in the β7-β8 insertion (H3 in DHR-1), which mediates extensive interactions with the HEAT/ARM repeats in PtdIns 3-kinase-γ, is common to both domains

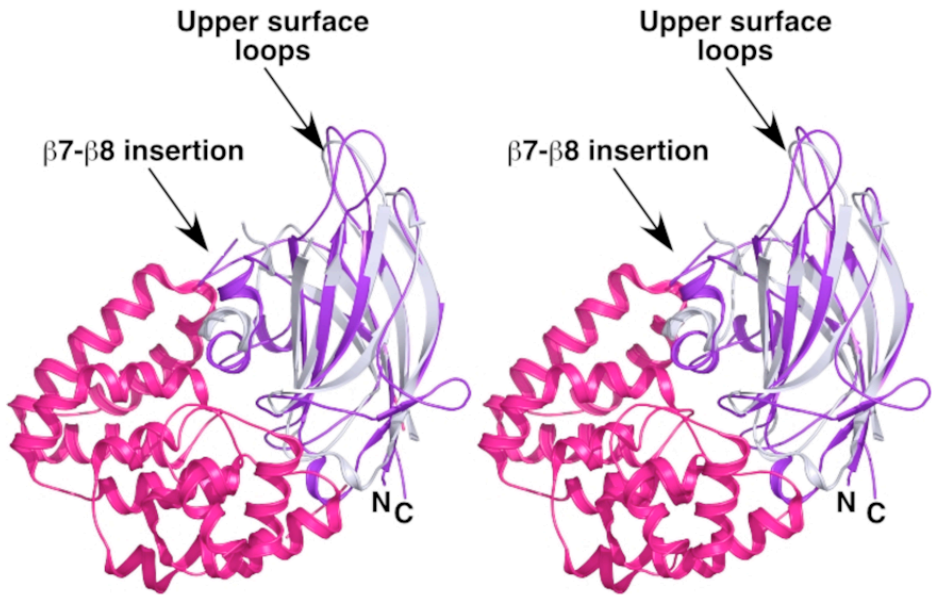

Figure S4. ITC titration curves for phosphilipid binding to DHR-1. (A—C) Representative ITC profiles: **(A)** 2 µl injections of 500 µM PtdIns(3,4,5)P_3 in 145 mM NaCl titrated into a cell containing 35 µM DHR-1. **(B)** 500 µM PtdIns(4,5)P_3 in 14 mM NaCl titrated into 35 µM DHR-1. **(C)** 500 µM Ins(1,3,4,5)P_4 into 25 µM DHR-1 **(D)** 584 µM PtdIns(4,5)P_2 into 35 µM DHR-1. **(E—F)** Competition assays. **(E)** 2 µl injections of 500µM PtdIns(3,4,5)P_3 titrated into pre-equilibrated PtdIns(4,5)P_2/DHR-1 (35 µM DHR-1 + 1.5-fold molar excess of PtdIns(4,5)P_2). **(F)** 2 µl injections of 582 µM PtdIns(4,5)P_2 titrated into pre-equilibrated PtdIns(3,4,5)P_3/DHR-1 (35 µM DHR-1 + a 1.5-fold molar excess of PtdIns(3,4,5)P_3).

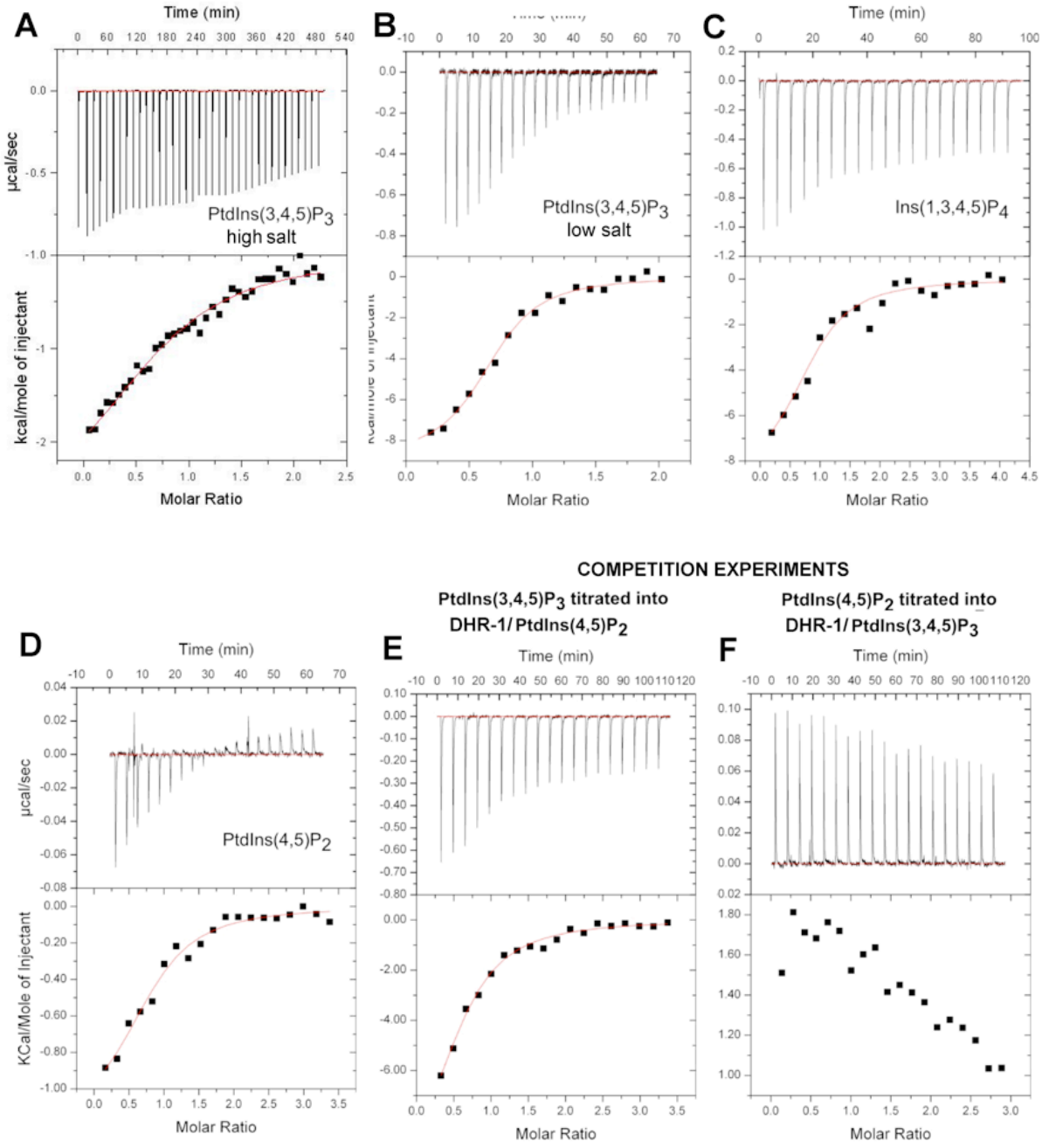

Figure S5. Surface electrostatic potentials comparing DHR-1 with other C2 domains. Top view looking down onto the surface loops of **(A)** calcium-independent and **(B)** calcium-dependent (left = calcium-free; right = calcium-bound) C2 domains. Electrostatic potentials calculated using APBS (Baker et al, 2001) and contoured at –5 kBT/e^- (red) and +5 kBT/e^- (blue). PTEN=1D5R; PtdIns3K-C2α=2B3R; Syn I C2A=1BYN; PKC-α= 3GPE.

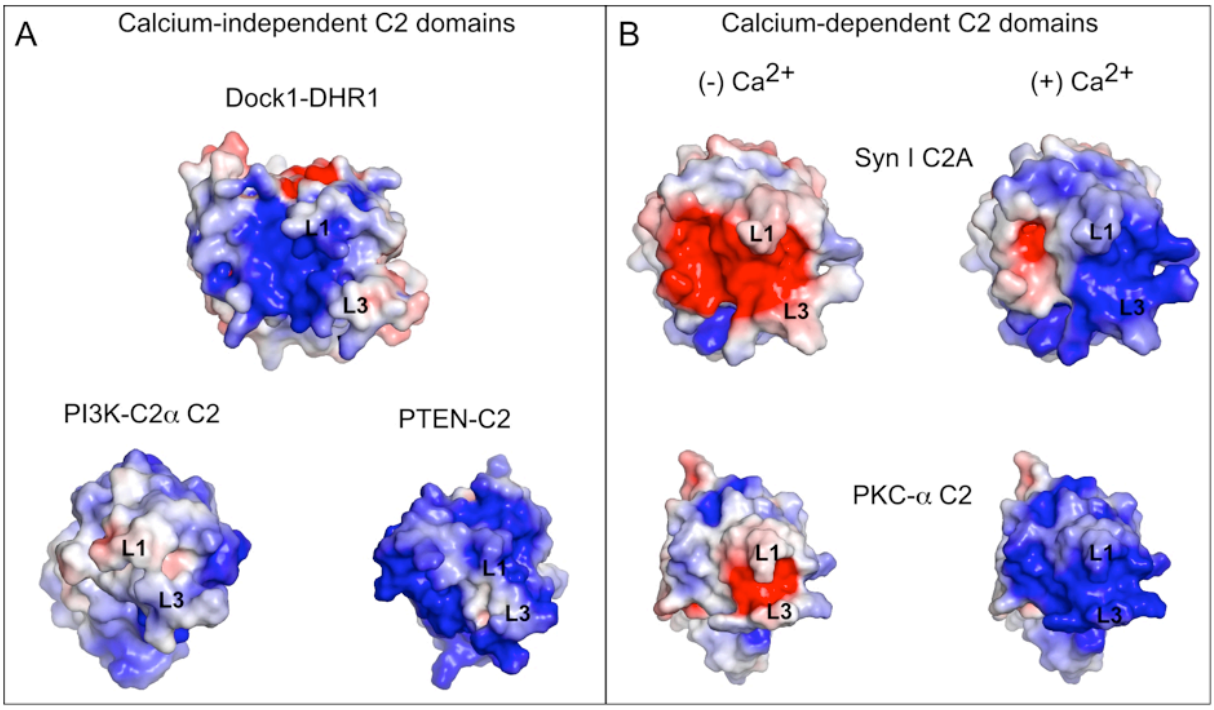

Figure S6. Computational docking of Ins(1,3,4,5)P_4 into DHR-1. **(A)** DHR-1 electrostatic surface map and the top 10 Ins(1,3,4,5)P_3 solutions as analyzed by 'Reranking Score' in Molegro Virtual Docker (Thomsen & Christensen, 2006). **(B)** Stereoview of 'top-ranked' PtdIns(3,4,5)P_3-binding mode prediction in the β-groove (note: we found no experimental evidence supporting binding at this site). Side chain flexibility was applied during the docking procedure, and conformations observed in the crystal structure (white) and after computational docking (green) are shown; see Material and Methods for details. A stereo image of Ins(1,3,4,5)P_4 docked into the upper surface loops is given in the main text (Fig. 5).

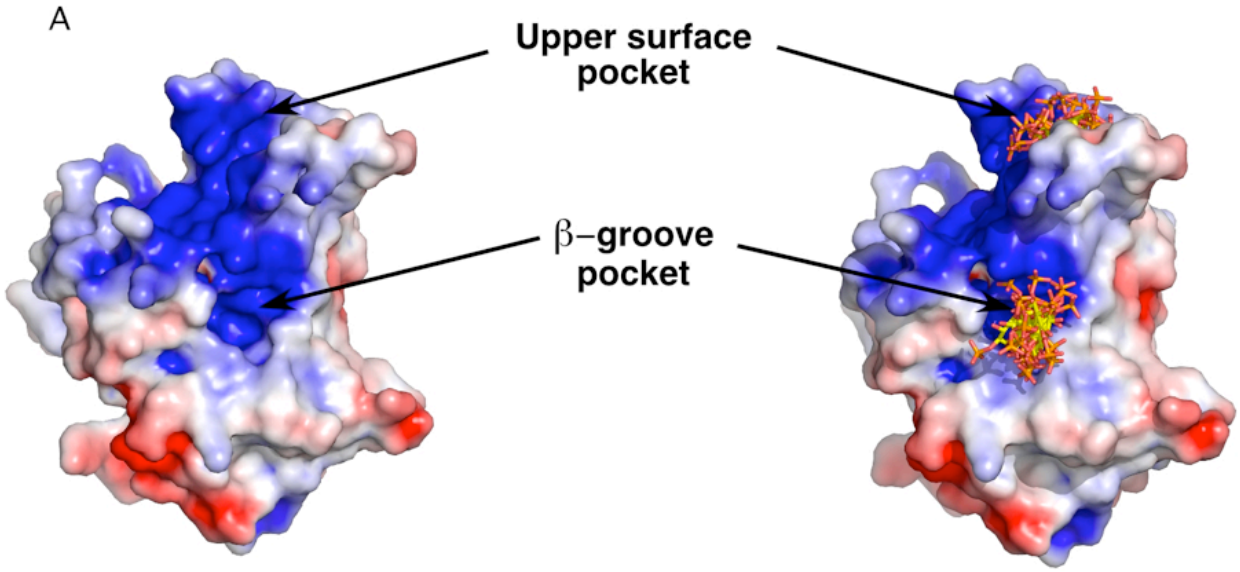

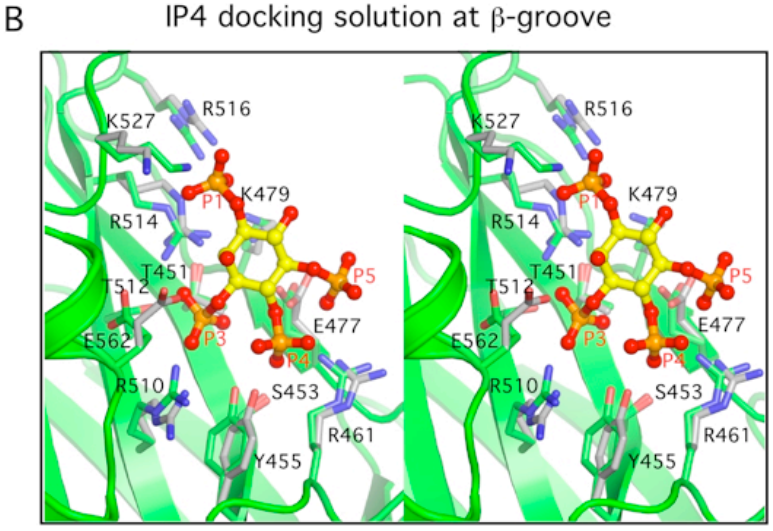

Figure S7. PtdIns(3,4,5)P_3-binding motifs in the Dock180 family. A detailed view of the L1 and L3 alignments. The central red boxes contains residues that may interact with the phosphoinositide head-group. Red-circled residues were mutated and shown to affect binding. With the exception of the beginning of L1 (which has an irregular conformation in Dock1), the loops show an alternating pattern of basic residues consistent with extended conformations that may present the (cyan-boxed) basic residues into the PtdIns(3,4,5)P_3 binding pocket. However, experimental verification is clearly required. Residues boxed in green have sidechains lining the β-groove, but mutations at these positions had no effect on phosphoinositide binding.

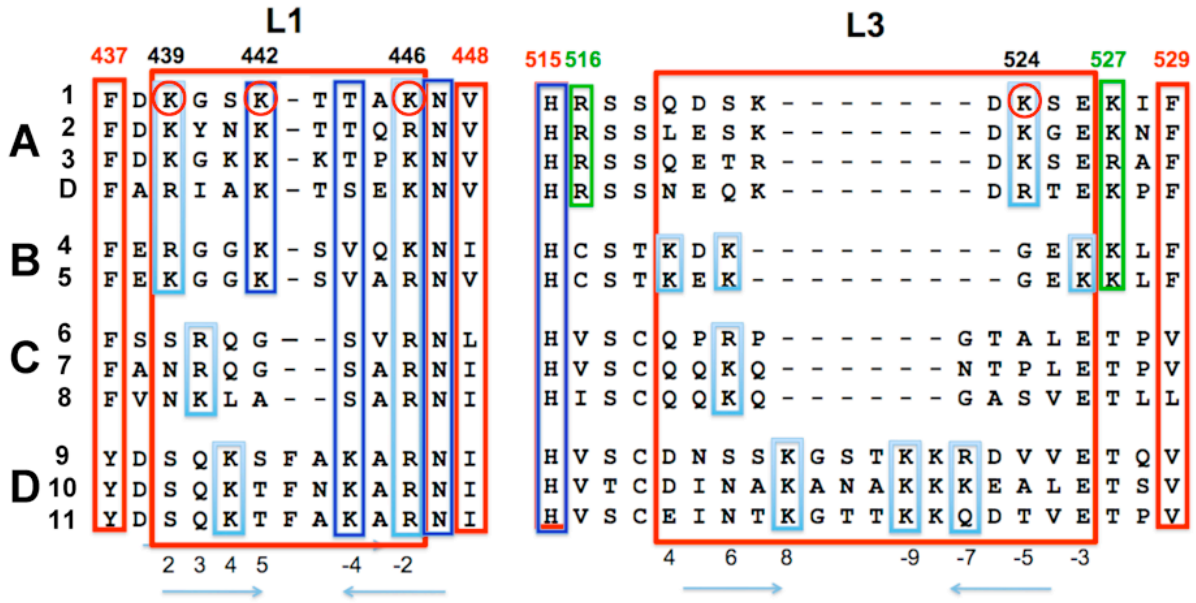

Figure S8. Stereoview of the putative phosphoinositide binding site in the Dock9 PH domain. (A) Superposition of the phosphoinositide binding sites of Dock9 (green) with Bruton's tyrosine kinase (yellow, PDB=1BWN) and DAPP1/PHISH (orange, PDB=1FAO). **(B)** Electrostatic surface potential of the Dock9 site, with Ins(1,3)P_2 modeled into site. Only the 3-phosphate is predicted to make strong interactions. The presence of F215 instead of the tyrosine found in other PH domains disfavors binding at the 4-phosphate position, by creating a steric clash with K182. A phosphate at the 5-position is predicted to be tolerated with little energetic consequence. The model is thus consistent with the observed preferences for PtdIns(3)P_1 and PtdIns(3,5)P_2 (Meller et al, 2008).

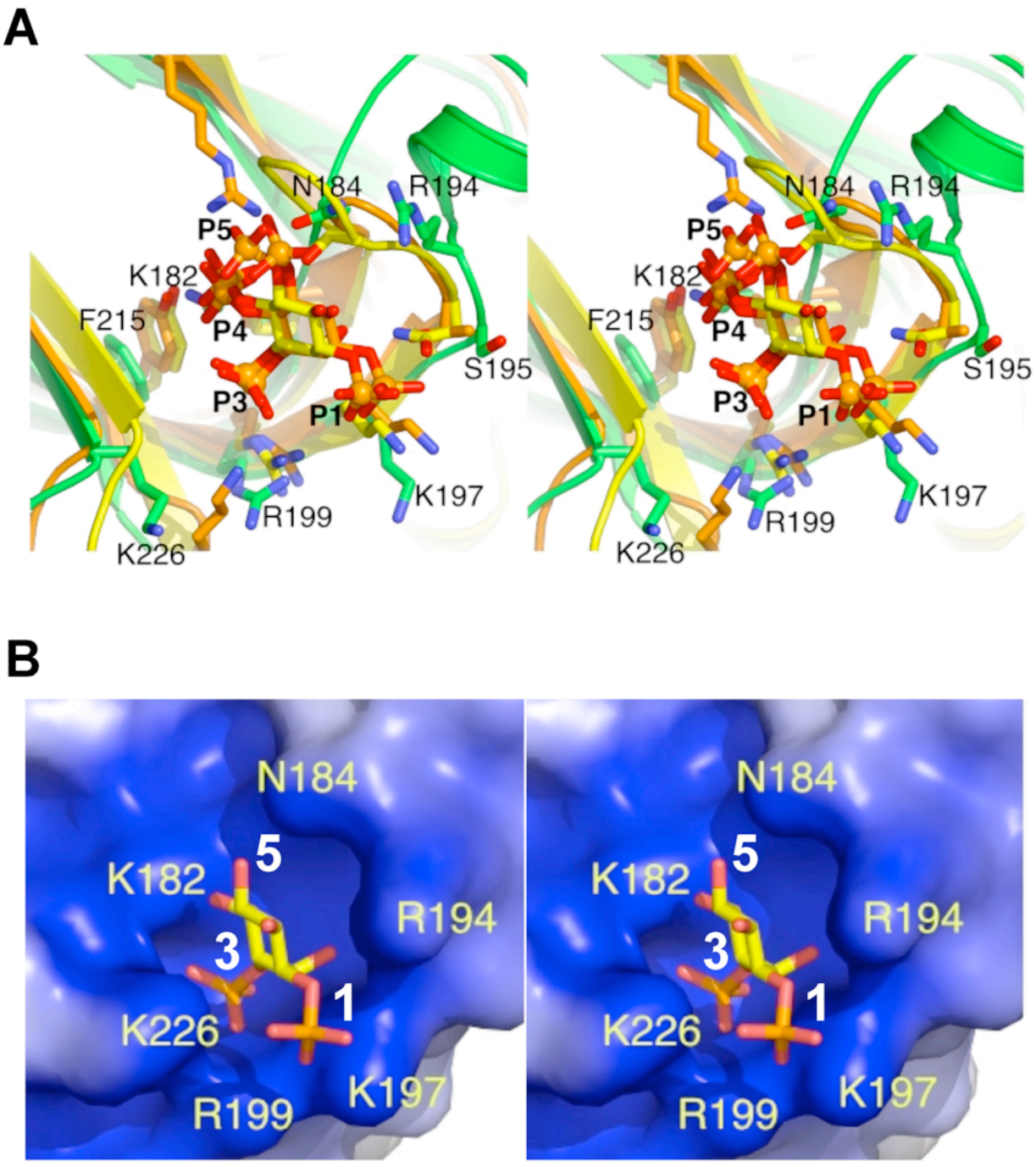

Figure S9. 3D-Jury predictions of an ARM-repeat domain between DHR-1 and DHR-2.

3D-Jury's top 18 unique hits based on the Dock1 sequence (residues 600–1200) are all ARM-repeat domains (classified by Families of Structurally Similar Proteins (FSSP) as 11.1.1 and by Structural Classification Of Proteins (SCOP) as a.118.1). The fold predictions accurately identify the DHR-1 and DHR-2 domain boundaries. 3DJury produces meta-predictions based on several prediction algorithms (3D-PSSM (Kelley et al, 2000), PDB-Basic (Ginalski et al, 2004b), FFAS03 (Rychlewski et al, 2000), Fugue (Rychlewski et al, 2000), mGenThreader (Jones, 1999a) and INUB (Fischer, 2003)), and scores models by their similarity to other models. Jscores above 50 indicate correct fold assignment with >90% probability (Ginalski et al, 2004a).

PP2A = Protein Phosphatase 2A; Ap1-β1 = Ap1 Clathrin Adaptor; [N] = Nuclear transport; [E] = Endocytosis; [S] = Scaffold protein

Fold Prediction Server	Jscore	PDB	Protein
FFAS03	157	1QGK	human importin-β [N]
INUB	157	1QGK	human importin-β [N]
3D-PSSM	150	1B3U	human PP2A-α[S]
INUB	149	2BKU	yeast importin-β [N]
mGenThreader	147	1QGR	human importin-β [N]
FFAS03	141	2BKU	yeast importin-β [N]
3D-Basic	138	1W63	mouse Ap1-γ [E]
Fugue	134	1QGR	human importin-β [N]
FFAS03	132	1W63	mouse Ap1-γ [E]
FFAS03	131	1UKL	mouse importin-β [N]
3D-Basic	127	1W63	mouse Ap1-β1 [E]
INUB	118	1W63	mouse Ap1-γ [E]
Fugue	114	1B3U	human PP2A-α[S]
mGenThreader	110	2BKU	yeast importin-β [N]
INUB	109	1B3U	human PP2A-α[S]
INUB	104	1W63	mouse Ap1-β1 [E]
mGenThreader	100	1B3U	human PP2A-α[S]
FFAS03	98	1OT8	human transportin-1 [N]

Figure S10. Secondary structure predictions for the DHR-1/DHR-2 interdomain region of Dock1. Predictions by Psipred (Jones, 1999b) and Profsec, an improved PHDsec (Rost, 1996), and Jpred3 (Cole et al, 2008), show a high correlation for residues 620 to 1210. The domain boundaries for DHR-1 and DHR-2 defined by crystal structures are highlighted in yellow and cyan. H=helix; E=strand; C=coil/loop

```
Dock1    DSFQISTLVCSTKLTQNVDLLGLLKWRSNTSLLQQNLRQLMKVDGGEVVKFLQDTLDALFNIMMENSESE

Psipred CEEEEEEEEEEEECCCHHHHHHHHHCCHHHHHHHHHHHCCCHHHHHHHHHHHHHHHHHHHCCCCC
Profsec CCEEEEEEEECCCCCCHHHHHHHHCCCCCHHHHHHHHHHHCCCHHHHHHHHHHHHHHHHHHHCCCCC
Jpred3  CEEEEEEEEEEEEECCCCHHHHHHHCCCCCHHHHHHHHHHCCCCCHHHHHHHHHHHHHHHHCCCCCC

Dock1    TFDTLVFDALVFIIGLIADRKFQHFNPVLETYIKKHFSATLAYTKLTKVLKNYVDGAEKPGVNEQLYKAM

Psipred CHHHHHHHHHHHHHHHHHHCCHHHHHHHHHHHHCCCCCCHHHHHHHHHHHHCCCCCCCCCHHHHHHH
Profsec HHHHHHHHHHHHHHHHHHCCCCCCCHHHHHHHHHCCCCCHHHHHHHHHHHHCCCCCCCHHHHHHHH
Jpred3  CCCCHHHHHHHHHHHCCCCCCCCHHHHHHHHCCCCEECCHHHHHHHHHHHHCCCCCCCHHHHHHHH

Dock1    KALESIFKFIVRSRILFNQLYENKGEADFVESLLQLFRSINDMMSSMSDQTVRVKGAALKYLPTIVNDVK

Psipred HHHHHHHHHHHHHHHHHHHCCCCCHHHHHHHHHHHHHHHHHHCCCCCHHHHHHHHHHHHHHHHHH
Profsec HHHHHHHHHHHHHHHHHHHCCCCCCCHHHHHHHHHHHHHHHHHCCCCCHHHHHHHHHHHHHHHHH
Jpred3  HHHHHHHHHHHHHHHHHHHHCCCCCHHHHHHHHHHHHHHHHHHCCCCCCCHHHHHHHHHHHHHHHH

Dock1    LVFDPKELSKMFTEFILNVPMGLLTIQKLYCLIEIVHSDLFTQHDCREILLPMMTDQLKYHLERQEDLEA

Psipred HHCCHHHHHHHHHHHCCCCCCHHHHHHHHHHHHHHCCCCCCCHHHHHHHHHHHHHHHHHCCCCHHHH
Profsec HCCCHHHHHHHHHHHHCCCCCCHHHHHHHHHHHHHCCCCCCCCHHHHHHHHHHHHHHHHCCCCHHHHH
Jpred3  HCCCHHHHHHHHHHHHCCCCCCHHHHHHHHHHHHHCCCCCCCCHHHHHHHHHHHHHHHHCCCHHHH

Dock1    CCQLLSHILEVLYRKDVGPTQRHVQIIMEKLLRTVNRTVISMGRDSELIGNFVACMTAILRQMEDYHYAH

Psipred HHHHHHHHHHHHHHCCCCCHHHHHHHHHHHHHHHHHHCCCCCCCCHHHHHHHHHHHHHHCCCCCCHHH
Profsec HHHHHHHHHHHHHHCCCCCCHHHHHHHHHHHHHHHHHHCCCCCCHHHHHHHHHHHHHHHCCCCCHHH
Jpred3  HHHHHHHHHHHHHCCCCCCCHHHHHHHHHHHHHHHHHHCCCCCCCCHHHHHHHHHHHHHCCCCCCCHH

Dock1    LIKTFGKMRTDVVDFLMETFIMFKNLIGKNVYPFDWVIMNMVQNKVFLRAINQYADMLNKKFLDQANFEL

Psipred HHHHCCCCCCCHHHHHHHHHHHHHHHCCCCCCCHHHHHHHHHHHHHHHHHHHHHHHHCCCCCHHHH
Profsec HHHHHCCCCHHHHHHHHHHHHHHHHHCCCCCCCCHHHHHHHHHHHHHHHHHHHHHHHHCCCCCHHH
Jpred3  CCCCCCCCCHHHHHHHHHHHHHHHHHCCCCCCCCHHHHHHHHHHHHHHHHHHHHHHHCCCCCCCHHH

Dock1    QLWNNYFHLAVAFLTQESLQLENFSSAKRAKILNKYGDMRRQIGFEIRDMWYNLGQHKIKFIPEMVGPIL

Psipred HHHHHHHHHHHHHCCCCCCCCCCCHHHHHHHHHHCHHHHHHHHHHHHHHHCCCCHHHHHHHHHHH
Profsec HHHHHHHHHHHHHCCCCCCCCCCCCHHHHHHHHHCCCHHHHHHHHHHHHHHHCCCCCCHHHHHHHHH
Jpred3  HHHHHHHHHHHHHCCCCCECCCCCHHHHHHHHHHHHHHHHHHHHHHHHHHHCCCCCCEEECCHHHHHH

Dock1    EMTLIPETELRKATIPIFFDMMQCEFHSTRSFQMFENEIITKLDHEVEGGRGDEQYKVLFDKILLEHCRK

Psipred HHHCCCCHHHHHCCHHHHHHHHHHHHHHCCCHHHHHHHHHHHHHHHHHCCCCCHHHHHHHHHHHHHHC
Profsec HEEECCCHHHHHHHHHHHHHHHHHHHHHCCCCCHHHHHHHHHHHHHHCCCCCCHHHHHHHHHHHHCC
Jpred3  HHCCCCCHHHHHHHHHHHHHHHHHHHHHHCCCHHHHHHHHHHHHHHHHCCCCCCCCCHHHHHHHHHCCCC

Dock1    HKYLAKTGETFVKLVVRLMERLLDYRTIMHDENKENRMSCTVNVLNFYKEIEREEMYIRYLYKLCDLHKE

Psipred CCCCCCCHHHHHHHHHHHHHHHHHHHHCCCCCCCCHHHHHHHHHHHHHHHCCCCHHHHHHHHHHHHHH
Profsec CCCCCHHHHHHHHHHHHHHHHHHHHHCCCCCCCCCCCCHHHHHHHHHHHHHHCCCHHHHHHHHHHHHHC
Jpred3  CCCCCHHHHHHHHHHHHHHHHHHHHHCCCCCCCCCCCCCHHHHHHHHHHHHHHCCCCCHHHHHHHHHHHH
```

References

Baker NA, Sept D, Joseph S, Holst MJ, McCammon JA (2001) Electrostatics of nanosystems: application to microtubules and the ribosome. *Proc Natl Acad Sci U S A* **98**(18)**:** 10037-10041

Cole C, Barber JD, Barton GJ (2008) The Jpred 3 secondary structure prediction server. *Nucleic Acids Res* **36**(Web Server issue)**:** W197-201

Fischer D (2003) 3D-SHOTGUN: a novel, cooperative, fold-recognition meta-predictor. *Proteins* **51**(3)**:** 434-441

Ginalski K, Kinch L, Rychlewski L, Grishin NV (2004a) BOF: a novel family of bacterial OB-fold proteins. *FEBS Lett* **567**(2-3)**:** 297-301

Ginalski K, von Grotthuss M, Grishin NV, Rychlewski L (2004b) Detecting distant homology with Meta-BASIC. *Nucleic Acids Res* **32**(Web Server issue)**:** W576-581

Holm L, Kaariainen S, Rosenstrom P, Schenkel A (2008) Searching protein structure databases with DaliLite v.3. *Bioinformatics* **24**(23)**:** 2780-2781

Jones DT (1999a) GenTHREADER: an efficient and reliable protein fold recognition method for genomic sequences. *J Mol Biol* **287**(4)**:** 797-815

Jones DT (1999b) Protein secondary structure prediction based on position-specific scoring matrices. *J Mol Biol* **292**(2)**:** 195-202

Kelley LA, MacCallum RM, Sternberg MJ (2000) Enhanced genome annotation using structural profiles in the program 3D-PSSM. *J Mol Biol* **299**(2)**:** 499-520

Meller N, Westbrook MJ, Shannon JD, Guda C, Schwartz MA (2008) Function of the N-terminus of zizimin1: autoinhibition and membrane targeting. *Biochem J* **409**(2)**:** 525-533

Rost B (1996) PHD: predicting one-dimensional protein structure by profile-based neural networks. *Methods Enzymol* **266:** 525-539

Rychlewski L, Jaroszewski L, Li W, Godzik A (2000) Comparison of sequence profiles. Strategies for structural predictions using sequence information. *Protein Sci* **9**(2)**:** 232-241

Thomsen R, Christensen MH (2006) MolDock: a new technique for high-accuracy molecular docking. *J Med Chem* **49**(11)**:** 3315-3321